

Subsurface non defect fatigue crack origin and local plasticity exhaustion

Guocai Chai^{1,2*}

¹ Strategy Research, Sandvik Materials Technology, 811 81 Sandviken, Sweden

² Engineering Materials, Linköping University, 581 83 Linköping, Sweden

* Corresponding author: guocai.chai@sandvik.com

Abstract Besides “fish eye”, subsurface non-defect fatigue crack origin (SNDFCO) in the matrix is another fatigue crack origin observed during very high cycle fatigue (VHCF). This paper provides some discussion on the phenomena and damage mechanisms from the recent investigations using four metallic materials with different microstructures. The results show that the strains in these materials in the VHCF regime were highly localized, especially in the multi-phase materials, where the local maximum strain can be eight times higher than the average strain value in the specimen. This high strain localization can lead to a fatigue damage or fatigue crack initiation at grain boundaries or twin boundaries by impingement cracking. High strain localization causes dislocation accumulation of very small strain during each cyclic loading and consequently the formation of local “fine grain area” and also increases the local hardness of the material. This can cause quasi-cleavage crack origin, and finally the formation of SNDFCO. The results in this paper indicate that fatigue damage and crack initiation mechanisms in the VHCF regime can be different in different metals due to the mechanisms for local plasticity exhaustion.

Keywords Very high cycle fatigue, Local plasticity exhaustion, Fatigue crack initiation, stainless steels

1. Introduction

Fatigue behaviors of metals in very high cycle fatigue (VHCF) regime have been widely investigated during the last decade [1-5]. It has been found that fatigue crack initiation in metals can shift from surface defects, subsurface defects and subsurface matrix with decreasing applied stress or increasing fatigue life [1, 4, 6]. Subsurface fatigue crack initiation has been mostly reported to start at subsurface defects such as inclusions, pores and microstructure inhomogeneity [4]. The surface treatments like shot peening, case hardening and surface nitriding can prevent the surface fatigue crack initiation, and cause a shift to a subsurface fatigue crack initiation at relatively higher stress amplitudes, and therefore improve the fatigue life or fatigue strength of the material [7]. Recently, another type of subsurface crack initiation, namely subsurface non-defect fatigue crack origin (SNDFCO), has been reported [6-8]. These crack origins were observed in the material fatigue tested for a very high fatigue life, and start in some phase or matrix of the material and are not associated with pre-existing defects.

In very high cycle fatigue regime, the applied stresses or strains are sometime well below the bulk yield strength or in the elastic deformation regime. How a cyclic plastic deformation or damage can occur in such a situation is still not well known. Hydrogen has been considered as a source for the formation of fish eye of subsurface inclusion [9], but this cannot explain a subsurface matrix crack initiation or formation of SNDFCO. Other mechanism such as localized deformation by dislocation pileup or grain boundary incompatibility has been proposed [6, 10]. These observations are however not enough to verify why SNDFCO has only been observed in some alloy systems. On the other hand, the mechanism for the shift of fatigue crack initiation from surface to subsurface is still not fully understood. Another phenomenon correlated to fatigue crack initiation in the VHCF regime is the formation of fine grains in the Fine Grain Area, FGA [11]. The reasons of the formation and the role of this FGA are not well explained either. In this investigation, fatigue crack initiation behavior and fatigue damage mechanism at a stress well below the bulk yield strength have been investigated in three metal materials with different microstructures using scanning electron microscopy, SEM, electron back scatter diffraction, EBSD and electron channel contrast

image, ECCI. The purposes are to get a better understanding of the mechanisms for sub-surface fatigue crack initiation in the matrix or formation of SNDFCO in the VHCF regime and the formation of FGA.

2. Materials and Experimental

2.1 Materials

Four metal materials: one nickel base alloy (Alloy 690), one martenistic–austenitic steel (MAS), one martensitic-ferritic (or bainite) steel (MFS), and one titanium alloy (Ti6Al4V), were used in this investigation. Table 1 and 2 show their nominal chemical compositions and mechanical properties.

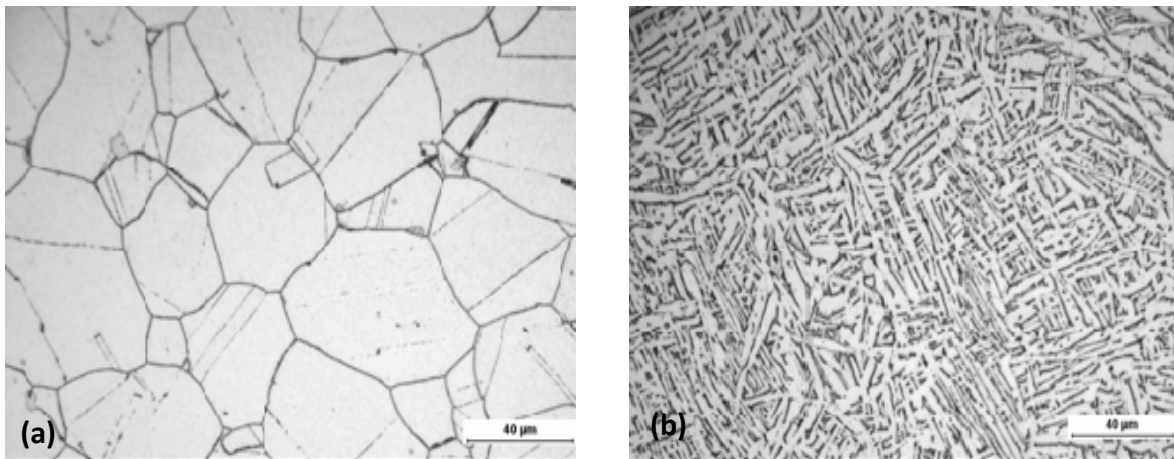
Table 1: Chemical compositions (wt%) and conventional tensile properties of the materials used

Alloy	C	Si	Mn	Cr	Ni	Ti	Fe	N	Mo	σ_{YT} (MPa)	σ_{UT} (MPa)
Alloy 690	0.018	0.30	0.27	29.6	58.85	0.26	10.51	0.026		305	582
MAS	0.38	0.4	0.6	13.5					1.0	1468	1968
MFS	0.23	0.25	0.65	1.3	2.7				0.25	986	1200

Table 2: Chemical composition (wt%) and conventional tensile property of titanium alloy

Alloy	C	Al	V	N	O	H	σ_{YT} (MPa)	σ_{UT} (MPa)
Ti 6Al4V	0,008	5.6	4.1	130ppm	940ppm	6ppm	876	952

Fig. 1 shows the microstructures of these four materials. Alloy 690 is a single phase material. The others are two or multi-phase materials. For MAS and MFS materials, the microstructures are very fine as shown in the TEM images.



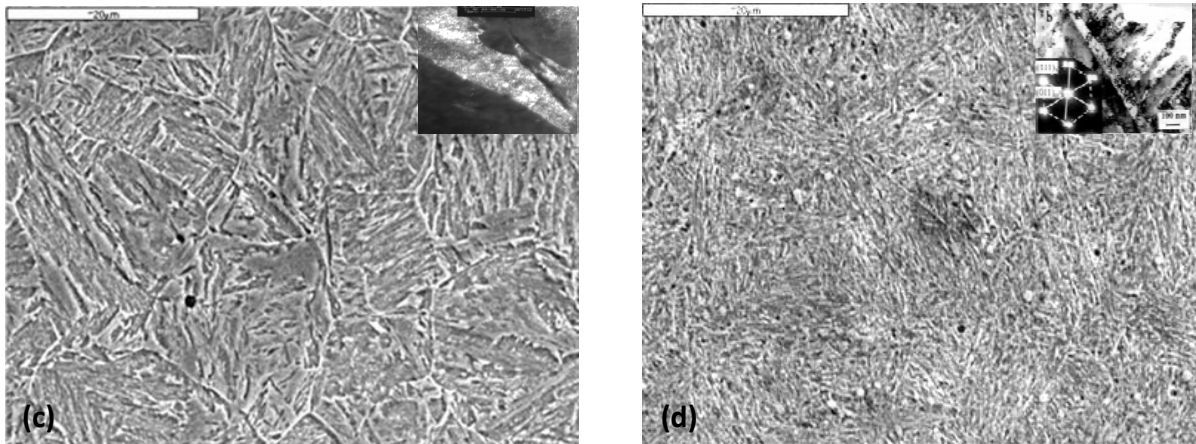


Fig. 1. Microstructures of the materials used for the fatigue tests. (a). Alloy 690, (b). Ti6Al4V, (c). Martensitic ferritic steel (MFS), (d). Martensitic austenitic steel (MAS).

2.2 Experimental

Two types of stress controlled fatigue tests have been carried out. One was performed using an Amsler machine with a frequency of about 140 Hz up to 5×10^8 cycles. Another test was performed using an ultrasonic (Piezo) fatigue testing machine with a frequency of 20 kHz up to 5×10^9 cycles. A round sample with a diameter up to 6mm was used. Pulsating tensile stresses with a stress ratio $R=0.1$ were applied for both tests.

The origins of fatigue crack initiation and fatigue pre-initiation damage (dislocation slip bands) were investigated using a JEOL 840 scanning electron microscope (SEM). In order to investigate the fatigue crack initiation mechanism and material damage process after the fatigue, the microstructures or damage in the samples after the VHCF testing were investigated using two scanning electron microscopy techniques: electron back scatter diffraction (EBSD) and electron channeling contrast image (ECCI). The EBSD technique was used to analyze the strain or stress localization or the influence of VHCF on the strain localization. Orientation maps were performed in a 6500 F JEOL field emission gun-scanning electron microscope (FEG-SEM) equipped with a TSL OIM EBSD system. EBSD maps were measured at 15 kV acceleration voltage and a working distance of 15mm. The ECCI technique has been recently proven as a powerful technique to image deformation damage and even dislocation structures steels by using a SEM [23]. ECCI observations were carried out in a Zeiss Crossbeam instrument (XB 1540, Carl Zeiss SMT AG, Germany) consisting of a Gemini type field emission gun (FEG) electron column and an focused ion beam (FIB) device (Orsay Physics). ECCI was performed at 10 kV acceleration voltage and a working distance of 5 mm, using a solid state 4-quadrant BSD detector. The microscope was run in the “high current” mode and an objective lens aperture of 120_μm was used.

3. Results and discussion

3.1 Fatigue life and crack initiation behavior

Fig. 2 shows the results of the fatigue tests for these four materials. The S-N curves use the applied stress amplitude versus number of cycles. Since these alloys have different strength, and therefore show different fatigue behaviors. Generally, the fatigue strength is related to the strength of the material.

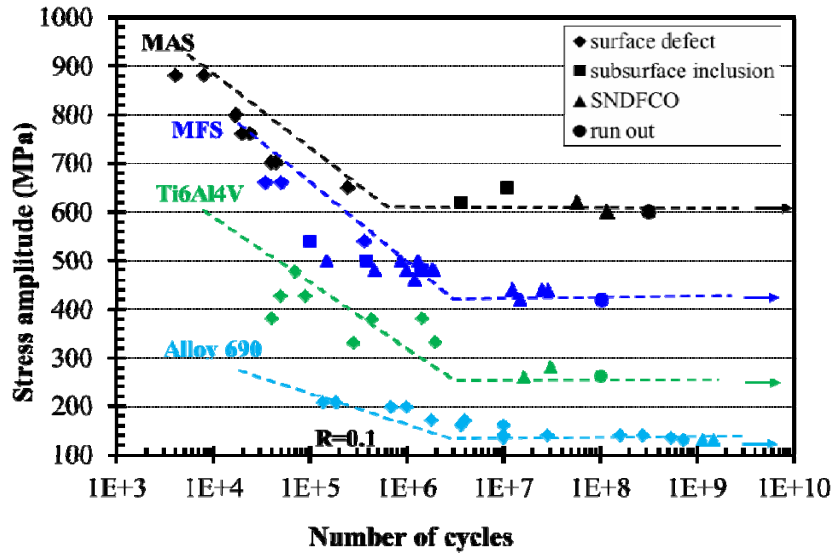
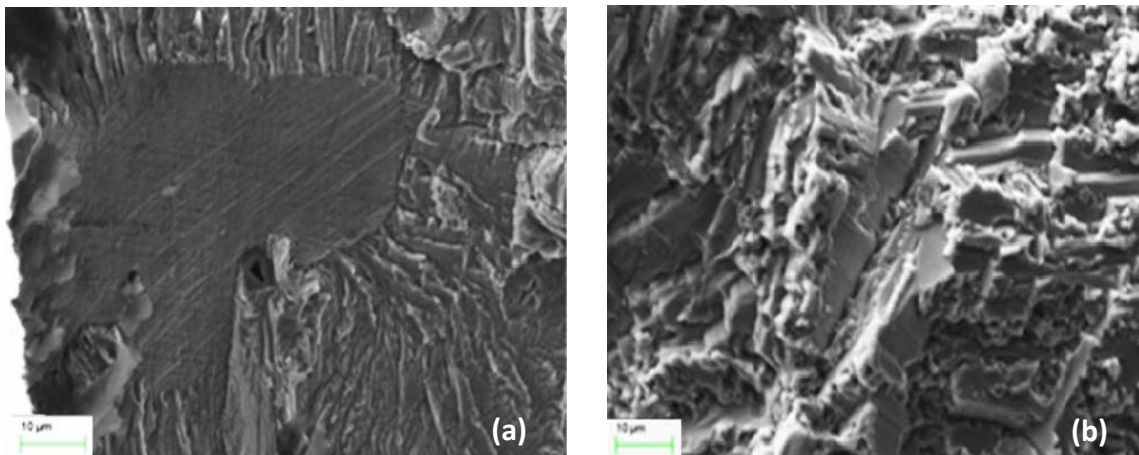


Fig. 2. S-N curves for four materials tested up to very high cycle fatigue regimes.

As expected, there is a shift of fatigue crack initiation from surface fatigue crack initiation (SFCO) to subsurface fatigue crack initiation (SDFCO) in all these four materials. With a further decrease of stress or a longer fatigue life, however, fatigue crack initiation at subsurface matrix (SFDFCO) can be observed. Four types of SNDFCO can be observed, which are shown in Fig. 3. The first type is a quasi-cleavage type of origin. They appear near the edge or inner of the sample (Fig. 3a). The second is that fatigue crack initiation at grain boundary or phase boundary, which becomes a rather small crack origin (Fig. 3b). The third is a facet type of origin, but small deformation slips on the fracture surface can be observed with a large magnification (small picture in Fig. 3c). The fourth is a small origin with lath type of microstructure. Rough surface can be observed. Usually, different alloys show different type of crack origins.



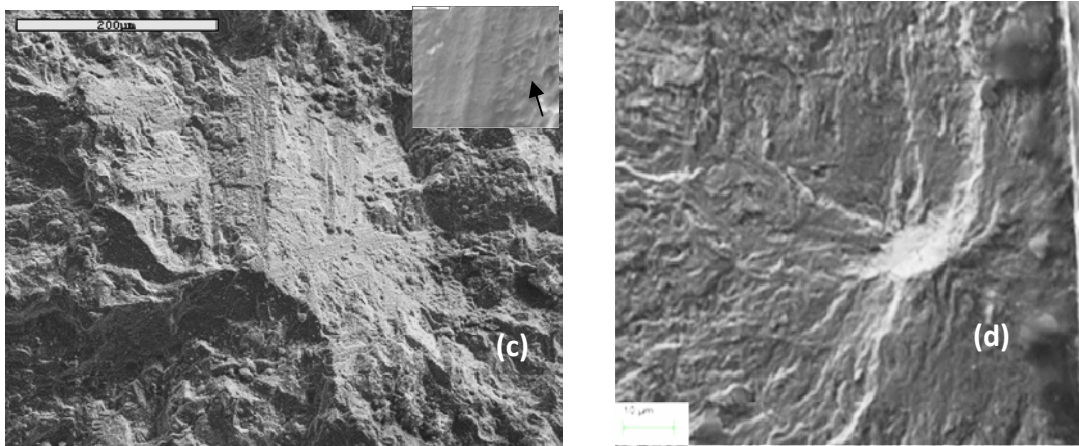


Fig. 3. Fatigue crack initiation in high cycle or very high cycle regime, (a). Alloy 690, quasi-cleavage, $\sigma_a=140\text{MPa}$, $N_f=1.61\times 10^8$, (b). Ti6Al4V, grain boundary, $\sigma_a=280\text{MPa}$, $N_f=3.0\times 10^7$, (c). Martensitic ferritic steel (MFS), facet, $\sigma_a=460\text{MPa}$, $N_f=1.2\times 10^6$, (d). Martensitic austenitic steel (MAS), lath, $\sigma_a=600\text{MPa}$, $N_f=3,2\times 10^8$.

3.2 Strain localization or plasticity exhaustion in very high cycle regime

In order to study the material damage mechanism in the VHCF regime, a special specimen was prepared by polishing the SNDFCO or fish eye. The local strains were then measured and evaluated using the EBSD technique. The local strain of each individual grain could be mapped through the image analysis of all the grains [12]. Fig. 4 shows the relative strains (strain contouring) for the specimens within SNDFCO or fish eye from Alloy 690, Ti6Al4V and MFS materials. A common character for these three specimens is that strain is very concentrated or localized (red color in the figures). Table 2 shows a comparison of the maximum strain and the average strain in SNDFCO or the views observed. The maximum strain is much higher than the average values. For MFS material, the maximum strain can be eight times higher than the average value. This indicates that the strain under SNDFCO is highly localized in this material.

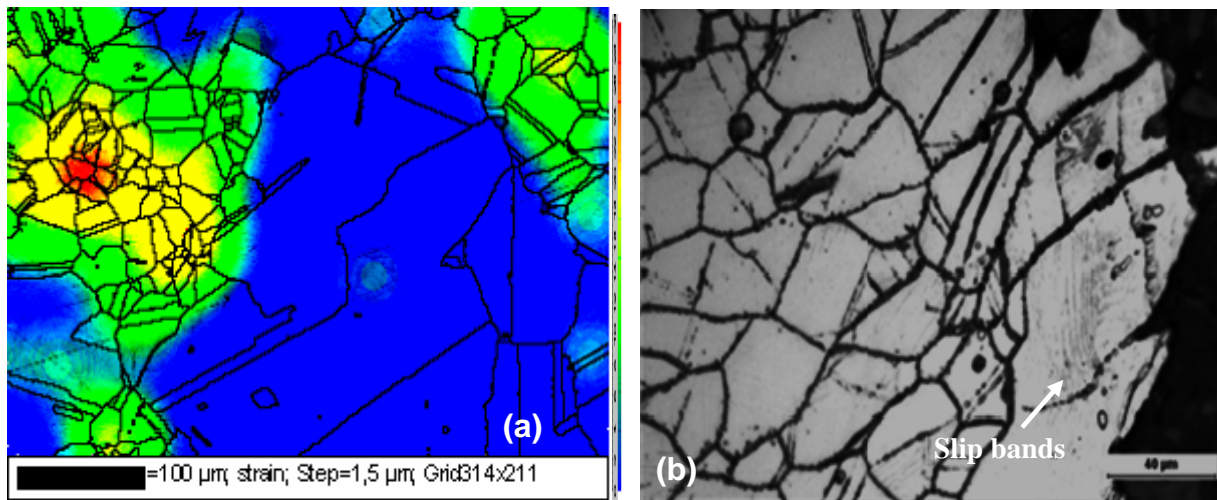


Figure 4. Strain contouring mappings obtained from EBSD analysis (a). Alloy 690 with $\Delta\sigma=135$ MPa, $N=5.45 \times 10^8$ cycles, (b). Alloy 690 with $\Delta\sigma=140$ MPa, $N=2.77 \times 10^8$ cycles.

Table 2. Maximum and average strain contouring from EBSD analysis of three materials

	MFS	Alloy 690	Ti6Al4V
Average	4,42	1,77	1,15
Maximum	36,46	9,35	3,76

MFS material, which has the highest strain localization (Table 2), has a hard martensitic phase and a soft ferritic phase. The soft phase could undertake cyclic plastic deformation at a stress even well below the bulk yield strength. This is because the applied stress can still be higher than the yield strength of the soft phase. The phase will thus undertake a cyclic plastic deformation, which can then cause a plasticity exhaustion and consequently formation of damage. SNDFCO is therefore formed for fatigue crack propagation. MAS material, which has a hard martensitic phase and a soft austenitic phase, has the similar situation. As known, strain localization can be related to accumulation of dislocations.

3.2 “Fine grains” in fatigue crack initiation area

Figure 5 shows the ECCI pictures under the fatigue crack initiation area (quasi-cleavage area) in Fig. 3a. Two types of microstructures can be identified. One is the “no or less deformation” area where is near the sample surface and center. Another is the area where “smaller or fine grains” can be observed (Fig. 5a). Actually, the area has high plastic deformation (Fig. 5b). “fine grains” have formed in some areas, but large plastic deformation can still be seen in other areas. This indicates that the formation of “fine grains” is a cyclic plastic deformation process, or formation of dislocation subcells. The size of “fine grains” depends on the stress concentration in the area and number of cycles. This phenomenon can explain the formation of FGA in the VHCF material reported earlier [11]. High stress concentration around the inclusion after giga numbers of cyclic loading can cause local dislocation initiation and movement, which cause the formation of dislocation subcells, and consequently the formation of fine grains.

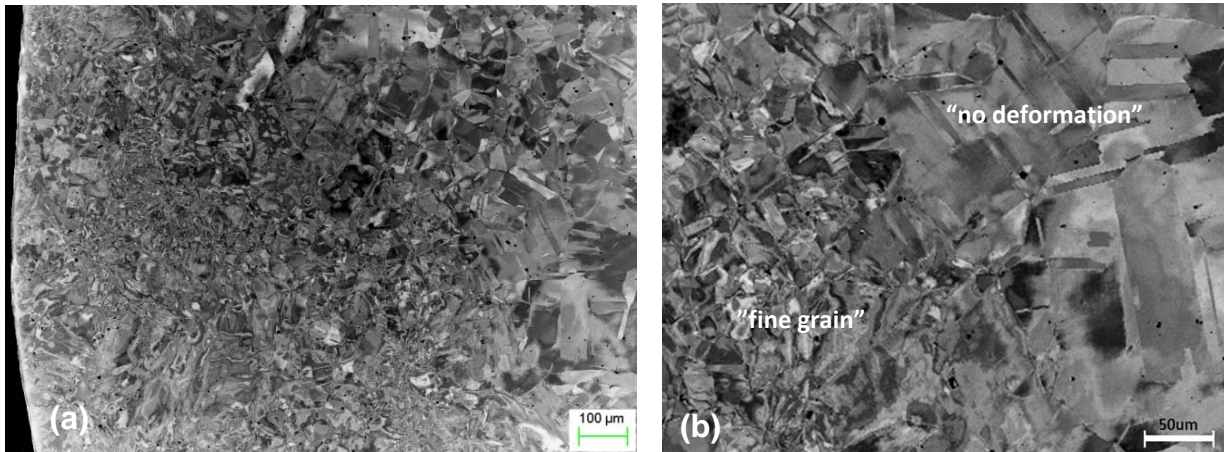


Figure 5. ECCI pictures show the microstructure under the fatigue crack initiation area in Fig. 3a, (a). Overview, (b). Enlarged (a).

In this “fine grain” area, high plastic deformation can be found (Fig. 6a). They are mainly appear near gran boundaries and twin boundaries. This may be attributed to dislocation pile-up as reported earlier [13]. Dislocation slip bands or eventually persistent slip bands (PSB) can be observed (Fig. 6b). They interact at grain boundaries and cause the formation of damage or micro crack due to impingement cracking. This observation shows that the fatigue crack initiation in the very high cycle fatigue regime can still compare with that in the low cycle fatigue regime [14].

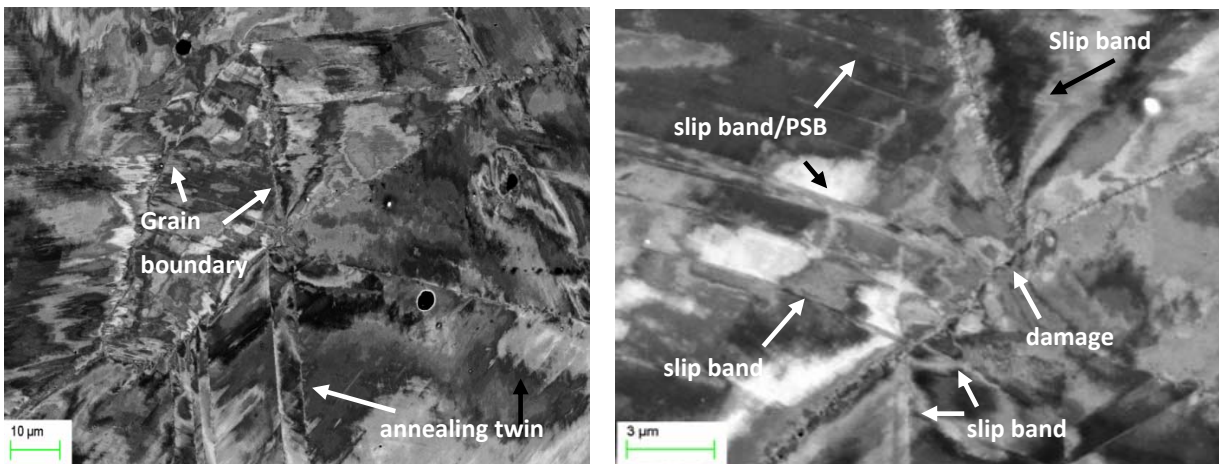


Figure 6 ECCI pictures show the microstructure under the fatigue crack initiation area in Fig. 3a, (a). Plastic deformation in the “fine grain, (b). Slip bands or PSB, interaction between slip band and grain boundaries.

As known, grain boundary or twin boundary act always as barriers to stop the movement of dislocations carried by slip bands, which leads to the formation of dislocation piling-up. Figures 7 shows that the twin boundary has blocked the movement of dislocations carried by slip bands, which cause the formation of damage at twin boundary due to the stress concentration by the piling-up of dislocations.

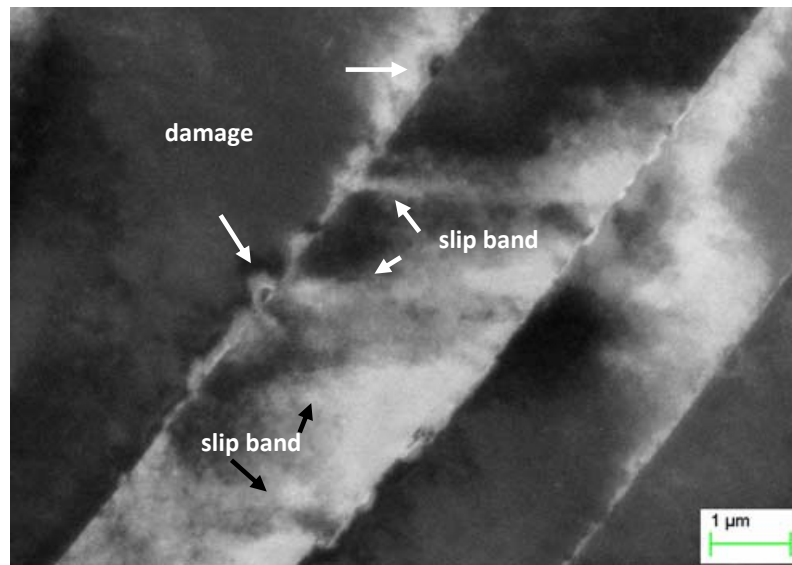


Figure 7 ECCI pictures show the microstructure under the fatigue crack initiation area in Fig. 3a, Formation of damage at twin boundary by dislocation slipping bands in the annealing twin.

The results discussed above are unexpected. High strain localization due to Schmid factor effect will cause an exhaustion of local plasticity of the material and dislocation slip band or persistent slip bands, and consequently formation of localized stress concentrations. This can lead to a fatigue damage or fatigue crack initiation at grain boundaries or twin boundaries by impingement cracking. High strain localization is the result of accumulation of very small strain during each cyclic loading in a much longer life or large number of cycles. This leads to the formation of local “fine grain area” and also increase the local hardness of the material, which can cause quasi-cleavage crack origin.

4. Size of SNDFCO

In this investigation, the formation of SNDFCO is treated as a crack propagation process. In the earlier work, the striations or ridges can be observed at the SNDFCO [6]. At small stress amplitudes, the striations can still be observed although the SNDFCO is facet (Fig. 3c). These striations are relatively small (50-100nm). The stress intensity factor ranges at the front of SNDFCO is evaluated using the following equation [15].

$$\Delta K = 0,5 \sigma_{\max} \sqrt{\pi \sqrt{area}} \quad (1)$$

In this study, $area=L*b$, where L is the maximum length of SNDFCO, and b is the shortest length of SNDFCO. This is a rather rough estimation since the actual SNDFCO is usually very irregular. Fig. 7 shows the stress intensity factor range at the front of SNDFCO in the martensitic-ferritic steel after the pulsating fatigue test. Although the size of SNDFCO is different, the stress intensity factor ranges at the front of SNDFCO are comparable, and vary from $2,8\text{MPa}\sqrt{\text{m}}$ to $4\text{MPa}\sqrt{\text{m}}$, which is in the range of the fatigue threshold values. For the martensitic-austenitic steel, the stress intensity factor range at the front of SNDFCO is between 3.17 to $3.33\text{MPa}\sqrt{\text{m}}$, which can compare with those of the

martensitic-ferritic phase alloy. These results show that the crack propagation within the SNDFCO is controlled by the microstructure mechanics, and the crack propagation outside the SNDFCO is controlled by elastic-plastic or linear mechanics. SNDFCO size depends on transition of crack propagation from stage I to stage II.

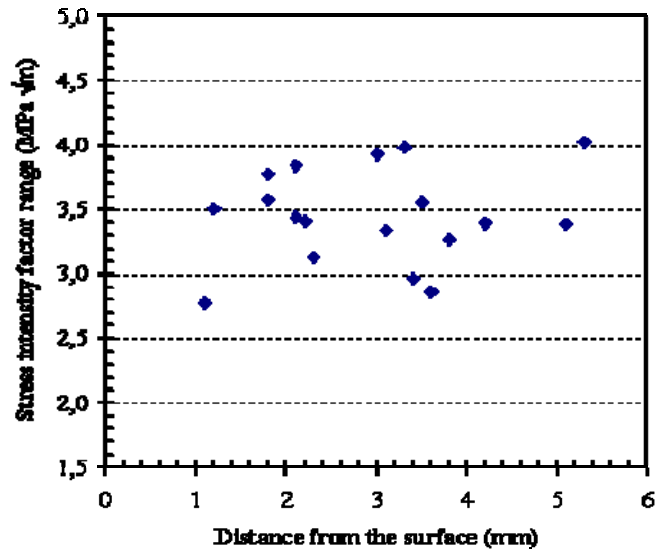


Figure 7. Stress intensity factor ranges at the front of SNDFCO in the martensite-ferritic steel.

5. Concluding remarks

In the VHCF regime, strain localization will occur in all these materials. This leads to local plasticity exhaustion the formation of local “fine grain area”. High strain localization causes dislocation accumulation of very small strain during each cyclic loading and consequently and also increases the local hardness of the material. This can cause quasi-cleavage crack origin, and finally the formation of SNDFCO.

The formation of SNDFCO is controlled by the microstructure mechanics. SNDFCO size depends on transition of crack propagation from stage I to stage II. The crack propagation outside the SNDFCO is controlled by elastic-plastic or linear mechanics.

Acknowledgements

This paper is published by permission of Sandvik Materials Technology. The author is also indebted to the co-authors in the reference list for their contribution and collaborations.

References

- [1] H. Mughrabi, *Fat. Fract. Eng. Mater Struct*, 25 (2002) 755.
- [2] P. Lukas and L. Kunz, *Fat. Fract. Eng. Mater Struct*, 25 (2002) 747.

- [3] C. Bathias and P. C. Paris, *Gigacycle fatigue in mechanical practice*, editor: Marcel Dekker, Section 7, (2004) ISBN 0-8247-2313-9.
- [4] Y. Murakami, *Metal Fatigue: Effect of small defects and non-metallic inclusion*, Elsevier Science Ltd, (2002).
- [5] Y. Gu, X. Teng, C. Liu, Y. He, C. Tao, *Acta Aeronautica et Astronautica Sinica*, 33 (2012), pp. 2136.
- [6] G. Chai, *International Journal of Fatigue*, 28 (2006) 1533.
- [7] O. Umezawa, and K. Nagai, *ISIJ International*. 37 (1997), pp. 1170-1179.
- [8] E. Notkina, G. Lütjering, and A. Gysler, *Proc. Inter. Conf. on Fatigue in the very High Cycle Regime*, University of Agriculture Science Press, (2001), Vienna, pp. 149-156.
- [9] Y. Murakami, T. Nomoto and T. Ueda, *Fat. Fract. Eng. Mater Struct*, 22 (1999) 581.
- [10] C. Stöcker, M. Zimmermann and H.-J. Christ, *International Journal of Fatigue*, 33 (2011) 2.
- [11] T. Sakai, W. Li, B. Lian and N. Oguma, *Review and new analysis on fatigue crack initiation mechanisms of interior inclusion – induced fracture of high strength steels in very high cycle regime*, (2011), *Proc. Of Conf. VHCF 5*, eds: D berger, H. –J. Christ, pp. 19.
- [12] N. Jia, R. Lin Peng, G. Chai, S. Johansson and Y. D. Wang, *Mater. Sci. and Eng. A* 491 (2008) 425.
- [13] G. Chai, N. Zhou, S. Ciurea, M. Andersson and R. Lin Peng, *Scripta Materialia* 66 (2012) p. 769.
- [14] P. Zhang, S. Qu, Q.Q. Duan, S.D. Wu, S.X. Li, Z.G. Wang and Z.F. Zhang, *Low-cycle fatigue-cracking mechanism in fcc crystalline materials*, *Philosophical Magazine*, Vol. 91, No. 2, 11 January 2011, 229–249.
- [15] Y. Murakami, *Eng. Frac. Mech.*, 22 (1985), pp. 101-114.